

Data Descriptor

Spatial Dataset for Comparing 3D Measurement Techniques on Lunar Regolith Simulant Cones

Piotr Kędziora¹ , Janusz Kobaka², Jacek Katzer² , Paweł Tysiąc³ , Marcin Jagoda^{1,*}  and Machi Zawidzki⁴ 

¹ Faculty of Civil Engineering, Environmental and Geodetic Sciences, Koszalin University of Technology, Śniadeckich 2, 75-453 Koszalin, Poland; piotr.kedziora@tu.koszalin.pl

² Faculty of Geoengineering, University of Warmia and Mazury in Olsztyn, Prawocheński 15, 10-720 Olsztyn, Poland; janusz.kobaka@uwm.edu.pl (J.K.); jacek.katzer@uwm.edu.pl (J.K.)

³ Faculty of Civil and Environmental Engineering, Gdańsk University of Technology, Gabriela Narutowicza 11/12, 80-233 Gdańsk, Poland; pawel.tysiacy@pg.edu.pl

⁴ Institute of Fundamental Technological Research, Polish Academy of Sciences, ul. Pawinskiego 5B, 02-106 Warsaw, Poland; zawidzki@ippt.pan.pl

* Correspondence: marcin.jagoda@tu.koszalin.pl

Abstract

The presented dataset contains spatial models of cones formed from lunar soil simulants. The cones were formed in a laboratory by allowing the soil to fall freely through a funnel. Then, the cones were measured using three methods: a high-precision handheld laser scanner (HLS), photogrammetry, and a low-cost LiDAR system integrated into an iPad Pro. The dataset consists of two groups. The first group contains raw measurement data, and the second group contains the geometry of the cones themselves, excluding their surroundings. This second group was prepared to support the calculation of the cones' volume. All data are provided in standard 3D file format (.STL). The dataset enables direct comparison of resolution and geometric reconstruction performance across the three techniques and can be reused for benchmarking 3D processing workflows, segmentation algorithms, and shape reconstruction methods. It provides complete geometric information suitable for validating automated extraction procedures for parameters such as cone height, base diameter, and angle of repose, as well as for further research into planetary soil and granular material morphology.

Dataset: <https://data.mendeley.com/datasets/z9bgmvtn5/1> (accessed on 26 December 2025)

Dataset License: CC BY 4.0



Academic Editor: Vladimir Sreckovic

Received: 3 December 2025

Revised: 31 December 2025

Accepted: 4 January 2026

Published: 6 January 2026

Copyright: © 2026 by the authors.

Licensee MDPI, Basel, Switzerland.

This article is an open access article distributed under the terms and conditions of the [Creative Commons](#)

[Attribution \(CC BY\) license](#).

1. Summary

Given the future development of planetary missions and human expansion onto the Moon's surface, the characteristics of lunar soil simulants are becoming a significant research topic, particularly in the context of construction technologies [1–4]. This dataset presents 3D measurement data of lunar regolith simulant cones acquired using three techniques: a handheld laser scanner, photogrammetry, and a LiDAR scanner integrated into an iPad. Each method represents a different level of precision, cost, and operational complexity,

and therefore making comparative evaluation essential for selecting technologies suitable for planetary soil analysis [5–9]. The data are the result of work related to research on lunar soil simulants (Chenobi, LHS-1, LMS-1, LSP-2) and CEN sand as a reference material. These materials have also been characterized in previous studies on lunar regolith simulants [10]. The original studies compared and evaluated how different acquisition methods cope with recording irregular surfaces on a small scale. Making the dataset available increases the value of the original article. Three-dimensional models are difficult to present in traditional manuscripts, so making them available is particularly important. Access to the data used in the original study allows other researchers to visualize, develop, and reinterpret the presented data. This allows for a more direct understanding of the limitations and advantages of each method described in the original article while providing potential for data reuse.

2. Data Description

The repository contains spatial data obtained from measuring cones formed from lunar regolith simulants, as well as granulometric data for the tested soils. The data are available in STL (.stl) and Excel (.xlsx) formats. The dataset consists of two main folders. “Raw” contains fifteen unprocessed mesh models representing the complete measurement scene after registration in the local coordinate system. Each material was measured using three techniques (HLS, photogrammetry, LiDAR), all aligned to a common coordinate system within that material’s dataset, but not between materials, as each represented a separate measurement setup. These meshes reflect the raw geometric data captured during measurement, retaining the original point density, measurement artifacts, and noise. “Cones” contains ten cropped and cleaned cone models. Each file includes only the cone geometry, isolated from its surroundings. These models were obtained from HLS and photogrammetry. Models from low-cost LiDAR scanning were not processed to this stage due to the limited precision of the method. Table 1 presents a summary of all available models, including the number of faces in each mesh and file sizes.

Table 1. Summary of mesh complexity and STL file size for each material and method.

Material	Device	Subset	Number of Faces	File Size [KB]
Chenobi	HLS	Raw	795,111	914,765
		Cone	215,424	237,746
	Photogrammetry	Raw	192,339	11,494
		Cone	47,308	2466
	Low-cost LiDAR	Raw	9269	453
		Cone	-	-
LHS_1	HLS	Raw	816,497	896,933
		Cone	281,511	325,188
	Photogrammetry	Raw	191,782	9851
		Cone	43,638	2208
	Low-cost LiDAR	Raw	9806	479
		Cone	-	-

Table 1. *Cont.*

Material	Device	Subset	Number of Faces	File Size [KB]
LMS_1	HLS	Raw	986,906	1,148,429
		Cone	315,738	371,244
	Photogrammetry	Raw	243,652	12,401
		Cone	34,108	1711
LSP_2	Low-cost LiDAR	Raw	8922	436
		Cone	-	-
	HLS	Raw	1,105,034	1,249,215
		Cone	295,754	347,120
CEN_Sand	Photogrammetry	Raw	160,155	7958
		Cone	35,864	1813
	Low-cost LiDAR	Raw	11,422	558
		Cone	-	-
	HLS	Raw	1,088,144	1,307,827
		Cone	419,684	470,398
	Photogrammetry	Raw	129,390	6410
		Cone	57,376	2871
	Low-cost LiDAR	Raw	10,200	499
		Cone	-	-

The file naming convention follows the format `xx_yy.stl`, where `xx`—corresponds to the name of the measurement method (HLS, Photogrammetry, LowCostLiDAR).

`yy`—represents the name of the measured regolith (Chenobi, LHS_1, LMS_1, LSP_2, CEN_sand).

Additionally, granulometric data obtained using a Bettersizer 2600 laser diffraction analyzer are provided in an Excel spreadsheet (Granulometric_Data.xlsx). These data include particle size distributions for each simulant and the reference material, measured using the Mie diffraction method.

3. Methods

The experiment consisted of four stages: granulometric analysis, cone creation, measurement, and post-processing. The lunar soil simulants used for the tests were Chenobi, LHS-1, LMS-1, and LSP-2. CEN quartz sand (PN-EN 196-1 [11]) was also used as a reference material. Before forming the cones, the granulometric properties of each material were tested. Measurements were performed using a Bettersizer 2600 laser diffraction analyzer (Bettersize Instruments Ltd., Dandong, China) the results are presented in Table 2. The cones were created by pouring each simulant through a funnel. The upper edge of the funnel was 287 mm above the pouring plane, and the lower edge was 172 mm above it. Each test used 250 mL of soil (measured before pouring). The exception was the Chenobi simulant, for which the volume was 150 mL due to its limited availability. For each test loose, uncompacted simulant was measured in a graduated beaker by gently pouring the material to the calibration mark, without tapping or compressing it. The test setup is illustrated in Figure 1. The measurements were performed under stable laboratory conditions. The ambient temperature was $20^{\circ}\text{C} \pm 0.5^{\circ}\text{C}$, and the relative humidity was $50\% \pm 1\%$.

Figure 2 shows an example of the final measurement setup. In addition to the cone, it shows the necessary measurement marks required for HLS measurements.

Table 2. Physical characteristics of the lunar regolith simulants and reference CEN sand (values based on manufacturer specifications).

Material	Manufacturer	Geological Analogue	Grain Size Percentiles (μm)	Loose Bulk Density (g/cm^3)
Chenobi	Deltion Innovations Ltd., Sudbury, ON, Canada	Lunar highlands	D3 = 3.2, D10 = 12.3, D50 = 62.5, D90 = 222.6	1.39
LHS-1	Space Resource Technologies, Oviedo, FL, USA	Lunar highlands	D3 = 4.0, D10 = 16.3, D50 = 96.2, D90 = 280.3	1.36
LMS-1	Space Resource Technologies, Oviedo, FL, USA	Lunar mare	D3 = 13.6, D10 = 40.2, D50 = 161.4, D90 = 428.2	1.62
LSP-2	Space Resource Technologies, Oviedo, FL, USA	Lunar south pole	D3 = 5.2, D10 = 21.7, D50 = 57.4, D90 = 401.7	1.45
CEN sand	Kwarcmix, Tomaszów Mazowiecki, Poland	Reference quartz sand	D3 = 126.7, D10 = 193.9, D50 = 815.7, D90 = 1544.0	1.5

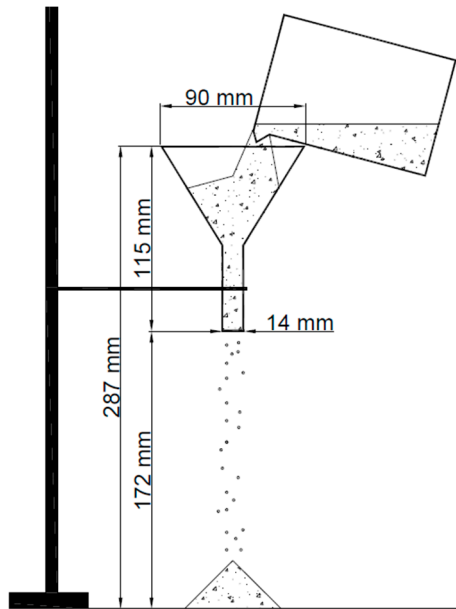


Figure 1. Schematic of the cone formation setup.

The measurement stage was carried out using three methods, in the following order: (1) HLS measurement, (2) photogrammetric measurement using an iPad, and (3) measurement using a LiDAR scanner integrated with an iPad. The first measurement was performed with a FreeScan Combo scanner from Shining 3D (Hangzhou, China). This measurement used blue light mode, which provides the device with a nominal accuracy of 0.02 mm. The minimum distance between model points was set to 0.1 mm. The distance between the scanner and the measured object was approximately 25 cm. The measurement was performed using the real-time data quality indicator provided by the scanner software (version 2.0.1.5). The measurement time for a single sample was approximately 10 min.

Afterward, the data required post-processing, which consisted of filling holes to create a watertight mesh. Processing the data took approximately 10 min and was carried out using the manufacturer's software (version 2.0.1.5). The resulting mesh models contained between 215,000 and 420,000 elements. This range depended on the roughness of the measured sample. Figure 3 shows an example of an HLS measurement result.



Figure 2. Scanning set-up for conducting measurements of LHS_1 LSS.

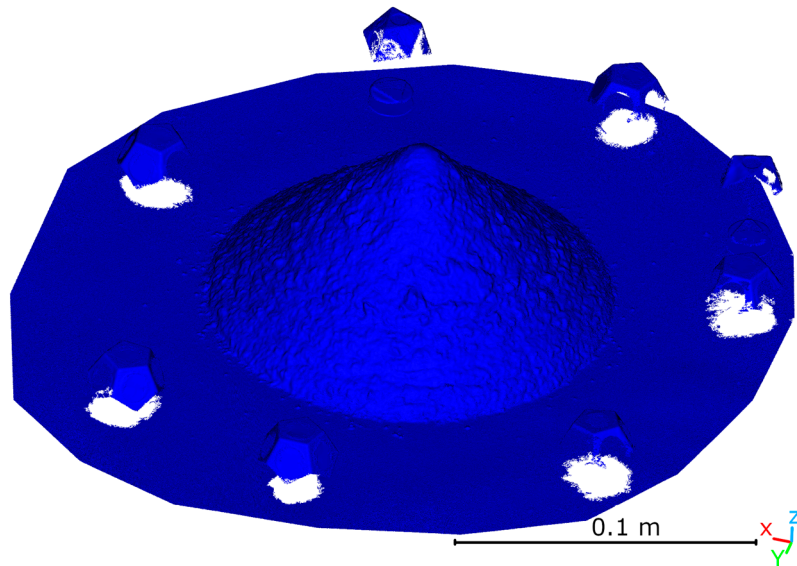


Figure 3. LHS-1 cone mesh measured by HLS.

Another dataset was acquired using close-range photogrammetry. The image source was the camera of an iPad Pro 2nd generation (Apple Inc., Cupertino, CA, USA). The Pix4Dcatch application (version 2.4.0) was used for image acquisition. The application controlled the exposure and ISO parameters, so the user could not adjust these settings manually. The measurement was performed by making three passes around each object and taking several photos from above. During the measurement, the device was positioned approximately 25 cm from the object. With a focal length of 4.15698 mm and a sensor pixel size of 0.0026 mm, a ground sampling distance (GSD) of 0.156 mm/pixel was achieved. The average measurement time for one sample was 5 min. The resulting image sets consisted of 150–200 photos and were processed using Agisoft Metashape software (version 1.8.5).

Image alignment was performed with high accuracy, dense point clouds were generated using high-quality depth maps, and mesh reconstruction was performed using the arbitrary surface type with a medium face count. The processing time for photos in photogrammetric software was 30 min. The number of mesh elements in the photogrammetric models ranged from approximately 34,000 to 57,000 faces. Figure 4 shows an example of a photogrammetric measurement result.

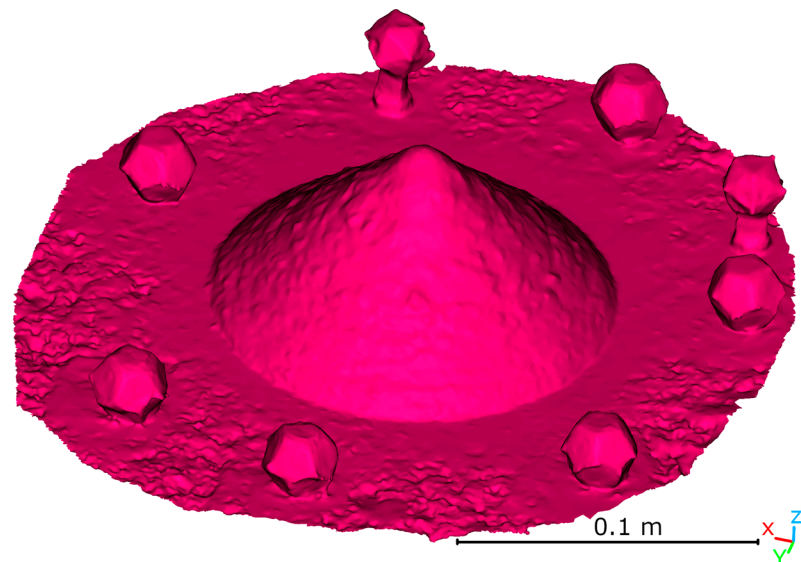


Figure 4. LHS-1 cone mesh measured by photogrammetry.

The last technology used was a low-cost LiDAR scanner, integrated into the 2nd generation iPad Pro (the same device used for photogrammetry). Measurements were performed with the 3DScannerApp (version 2.1.3). The measurements were taken in three passes. For the upper part of the cone, data were acquired from above, similar to the photogrammetric approach. Each measurement took about three minutes. Afterward, post-processing was performed using the same application. The voxel size was set to the minimum value of 4 mm, smoothing was disabled, and the model was simplified by 20%. Post-processing each sample took approximately 3 min. The resulting meshes contained between 2500 and 4500 faces. Figure 5 shows an example of a low-cost LiDAR measurement result.

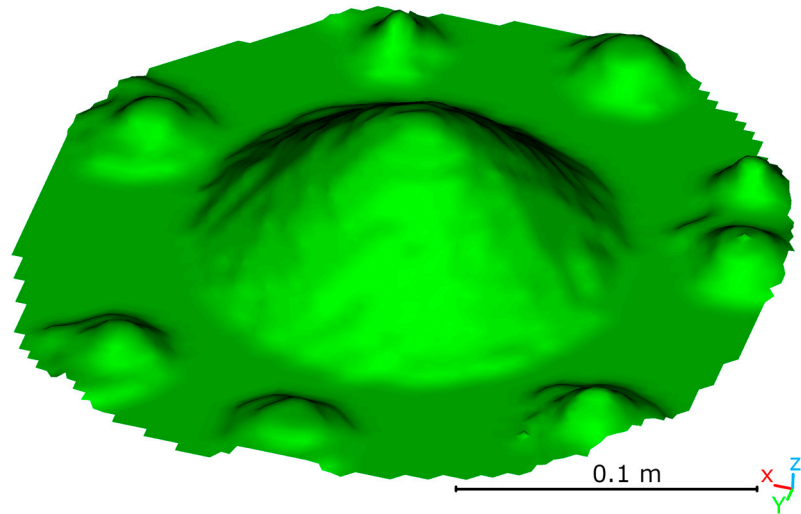


Figure 5. LHS-1 cone mesh measured by low-cost LiDAR.

Although the meshes obtained with the low-cost LiDAR scanner contain far fewer faces than those obtained with HLS or photogrammetry, they still constitute meaningful test data. They can be used to evaluate the robustness of segmentation and base-detection algorithms under strongly undersampled conditions. They can also be used to benchmark sensor-fusion workflows by combining coarse LiDAR with high-resolution HLS or photogrammetric models. Additionally, they can be used to study how decreasing spatial resolution propagates into errors in the estimation of basic geometric parameters. Therefore, the dataset offers a realistic example of the level of geometric detail that can be expected from mobile LiDAR sensors when applied to small, granular targets.

All 3D datasets were subsequently processed using CloudCompare (version 2.13.1) for registration and alignment. The cleaning and trimming of individual cone models were performed in CloudCompare and Blender (version 4.1). To obtain trimmed, cone-only meshes from the raw measurement scenes, a cutting plane at a defined height (Z) was used. First, a base plane representing the flat support surface on which the cone was formed was estimated for each dataset by fitting a plane to the points in the surrounding ground area. Then, the elevation of this plane was transferred to Blender and used as a reference cutting plane. Each mesh was clipped so that all geometry located below the reference plane and a thin layer up to 0.02 mm above it were removed, closing the cone base and simultaneously producing a watertight model. Next, all loose grains captured during scanning that did not belong to the cone body were identified and deleted. These grains were separate geometric components not connected to the cone volume. This left only the cleaned cone geometry.

As a simple example of how the meshes can be used, basic geometric parameters can be derived directly from the models. The height of a cone can be obtained as the vertical distance between the apex and the fitted base plane, while the base diameter can be calculated from a circular fit to a suitably selected section of the model. In the companion research article [1], this workflow was applied to all cones. Across all materials, handheld laser scanning and photogrammetry yielded very similar results, with mean absolute differences of 0.5 ± 0.4 mm for cone height, 0.4 ± 0.2 mm for base diameter, and $0.15 \pm 0.14^\circ$ for angle of repose. In contrast, the iPad LiDAR systematically underestimated cone heights by 9.1 ± 2.9 mm and overestimated base diameters by 9.6 ± 6.1 mm, leading to angle deviations of $2.63 \pm 0.97^\circ$. For instance, for the Chenobi simulant, the difference in cone height between HLS (53.5 mm) and photogrammetry (53.2 mm) was 0.3 mm, whereas the iPad LiDAR (43.8 mm) underestimated the height by about 10 mm. For the base diameter, the differences were 1 and 17 mm, respectively [1].

Author Contributions: Conceptualization, P.K., J.K. (Janusz Kobaka), J.K. (Jacek Katzer), P.T., M.J. and M.Z.; methodology, P.K., J.K. (Janusz Kobaka), J.K. (Jacek Katzer), P.T., M.J. and M.Z.; software, P.K., J.K. (Janusz Kobaka), J.K. (Jacek Katzer), P.T., M.J. and M.Z.; validation, P.K., J.K. (Janusz Kobaka), J.K. (Jacek Katzer), P.T., M.J. and M.Z.; formal analysis, P.K., J.K. (Janusz Kobaka), J.K. (Jacek Katzer), P.T., M.J. and M.Z.; investigation, P.K., J.K. (Janusz Kobaka), J.K. (Jacek Katzer), P.T., M.J. and M.Z.; resources, P.K., J.K. (Janusz Kobaka), J.K. (Jacek Katzer), P.T., M.J. and M.Z.; data curation, P.K., J.K. (Janusz Kobaka), J.K. (Jacek Katzer), P.T., M.J. and M.Z.; writing—original draft preparation, P.K., J.K. (Janusz Kobaka), J.K. (Jacek Katzer), P.T., M.J. and M.Z.; writing—review and editing, P.K., J.K. (Janusz Kobaka), J.K. (Jacek Katzer), P.T., M.J. and M.Z.; visualization, P.K., J.K. (Janusz Kobaka), J.K. (Jacek Katzer), P.T., M.J. and M.Z.; supervision, P.K., J.K. (Janusz Kobaka), J.K. (Jacek Katzer), P.T., M.J. and M.Z.; project administration, P.K., J.K. (Janusz Kobaka), J.K. (Jacek Katzer), P.T., M.J. and M.Z.; funding acquisition, P.K., J.K. (Janusz Kobaka), J.K. (Jacek Katzer), P.T., M.J. and M.Z. All authors have read and agreed to the published version of the manuscript.

Funding: This research received no external funding.

Institutional Review Board Statement: Not applicable.

Informed Consent Statement: Not applicable.

Data Availability Statement: The data presented in the study are openly available at <https://data.mendeley.com/datasets/z9bgmvtmg5/1> (accessed on 26 December 2025).

Conflicts of Interest: The authors declare no conflicts of interest.

References

1. Kędziorański, P.; Kobaka, J.; Katzer, J.; Tysiak, P.; Jagoda, M.; Zawidzki, M. Comparison of spatial data acquisition techniques for the geometric analysis of lunar regolith. *Measurement* **2026**, *258*, 119366. [\[CrossRef\]](#)
2. Ishii, T.; Kioka, A.; Huang, J.-J.S.; Tsuji, T.; Yamada, Y. Distinctive impact responses of extraterrestrial regolith simulants: Insights from crater morphology classification and granular dynamics through machine learning and x-ray computed tomography. *Phys. Fluids* **2025**, *37*, 023358. [\[CrossRef\]](#)
3. Zhang, T.; Chao, C.; Yao, Z.; Xu, K.; Zhang, W.; Ding, X.; Liu, S.; Zhao, Z.; An, Y.; Wang, B.; et al. The technology of lunar regolith environment construction on Earth. *Acta Astronaut.* **2021**, *178*, 216–232. [\[CrossRef\]](#)
4. Kobaka, J.; Katzer, J.; Seweryn, K. Magnetic Separation of Lunar Regolith as its Beneficiation for Construction Effort on the Moon. *Artif. Satell.* **2023**, *58*, 203–213. [\[CrossRef\]](#)
5. Monsalve, A.; Yager, E.M.; Tonina, D. Evaluating Apple iPhone LiDAR measurements of topography and roughness elements in coarse bedded streams. *J. Ecohydraulics* **2025**, *10*, 181–191. [\[CrossRef\]](#)
6. Nakamura, T.; Kioka, A.; Egawa, K.; Ishii, T.; Yamada, Y. Estimating millimeter-scale surface roughness of rock outcrops using drone-flyover structure-from-motion (SfM) photogrammetry by applying machine learning model. *Earth Sci. Inform.* **2024**, *17*, 2399–2416. [\[CrossRef\]](#)
7. Kędziorański, P.; Jagoda, M.; Tysiak, P.; Katzer, J. An Example of Using Low-Cost LiDAR Technology for 3D Modeling and Assessment of Degradation of Heritage Structures and Buildings. *Materials* **2024**, *17*, 5445. [\[CrossRef\]](#) [\[PubMed\]](#)
8. Huang, X.; Zhu, F.; Wang, X.; Zhang, B. Automatic Measurement of Seed Geometric Parameters Using a Handheld Scanner. *Sensors* **2024**, *24*, 6117. [\[CrossRef\]](#) [\[PubMed\]](#)
9. Ruiz, R.M.; Torres, M.T.M.; Allegue, P.S. Comparative Analysis Between the Main 3D Scanning Techniques: Photogrammetry, Terrestrial Laser Scanner, and Structured Light Scanner in Religious Imagery: The Case of The Holy Christ of the Blood. *J. Comput. Cult. Herit.* **2021**, *15*, 18. [\[CrossRef\]](#)
10. Kafka, O.L.; Moser, N.H.; Chiaramonti, A.N.; Garboczi, E.J.; Wilkerson, R.P.; Rickman, D.L. Measurement of the three-dimensional shape and size distribution of 17 lunar regolith simulants: Simulant shape and size inter-comparison and simulant shape comparison with Apollo 11 and Apollo 14 lunar regolith. *Icarus* **2025**, *434*, 116542. [\[CrossRef\]](#)
11. PN-EN 196-1:2016-07; Methods of Testing Cement—Part 1: Determination of Strength. Polish Committee for Standardization: Warsaw, Poland, 2016.

Disclaimer/Publisher's Note: The statements, opinions and data contained in all publications are solely those of the individual author(s) and contributor(s) and not of MDPI and/or the editor(s). MDPI and/or the editor(s) disclaim responsibility for any injury to people or property resulting from any ideas, methods, instructions or products referred to in the content.